Materials and Design 50 (2013) 997–1004

Contents lists available at SciVerse ScienceDirect

Materials and Design

journal homepage: www.elsevier.com/locate/matdes

Technical Report

Tribological behaviour of near β titanium alloy as a function of α + β solution treatment temperature

Srinivasu Gangi Setti *, R.N. Rao

Department of Mechanical Engineering, National Institute of Technology, Warangal 506 021, India

ARTICLE INFO

Article history:
Received 1 February 2013
Accepted 30 March 2013
Available online 11 April 2013

ABSTRACT

The Ti–10V–4.5Fe–3Al alloy is one of the recently developed low cost near beta titanium alloy. In this study, the effect of α + β solution treatment temperature on the microstructure and sliding wear properties of Ti–10V–4.5Fe–Al were evaluated. A pin on disc apparatus is used for the testing according to ASTM standard (G99). The volume fraction of α decreases with increase in α + β solution treatment temperature. The %weight loss is decreasing with the decrease in α + β solution treatment temperature. ANOVA analysis is also carried out to know the influence of input parameters on the out parameters. Load and sliding distances are the main contributing parameters and also α + β solution treatment temperature having the influence.

1. Introduction

Titanium alloys are having very good characteristics like less weight, high strength to weight ratio, excellent elevated temperature properties, good corrosion resistance, etc. [1,2]. Because of these advantages titanium alloys are used in aerospace, automotive, chemical, marine, energy applications, etc. [3–6]. These alloys also possess very good bio-compatibility with human body fluids and they are used in biomedical applications [7,8]. However, titanium alloys are known for their disreputably poor tribological properties [9,10]. This issue may limit their applicability particularly in areas involving wear and friction. Two main factors have been suggested as responsible for the poor tribological properties of titanium alloys [10]: 1. Low resistance to plastic shearing and low work hardening, and 2. Low protection exerted by the surface oxide which may form as a consequence of the high flash temperature induced by frictional heating.

In order to improve the tribological properties different techniques are adopted. Those are surface modification, composition adjustment, heat treatment, reinforcing the matrix with some hard precipitates, etc. Most of the research work in tribological field is only on Ti–6Al–4V [11,12] and very limited literature is available in Ti alloys other than Ti–6Al–4V [13–15]. The present study of the work is the tribological behaviour of the recently developed low cost near beta titanium alloy in different α + β solution treatment conditions. Analysis of Variance (ANOVA) is one of the most commonly used statistical methods. The purpose of ANOVA analysis is to know which parameter is significantly affecting the sliding wear properties. Most of the researchers have used this method along with the taguchi technique [16–19] for to study the tribological behaviour of composite materials [20]. The frictional behaviour is also studied in this work because the coefficient of friction is also an important parameter in biomedical applications.

2. Materials and methods

2.1. Material

Ti–10V–4.5Fe–3Al ingot having a diameter of 145 mm was fabricated by vacuum arc remelting method. The β transus temperature of the alloy (T_β) was determined is 780 °C in close agreement with the value of β transus for the alloy as per Yolton's formula [21]. The alloy was thermo-mechanically (forging and rolling) processed to get the equi axed α particles in β phase. Thermo-mechanical process includes forging and rolling as previously mentioned. The ingot was then forged at 900 °C (β forging) to a 15 mm thick slab. Further it was rolled into 10 mm thick slab at 750 °C (α–β rolling). Table 1 shows the chemical composition of the alloy.

2.2. Microscopy

After different α + β solution treatments at 750, 720, and 680 °C, specimens of 15 mm × 15 mm × 5 mm dimension were cut and mounted for microstructural examination. The heat treatment was carried out in the electric heat treatment furnace. Microstructures of the alloy were examined and characterised, using scanning electron microscopy. The specimens for the optical microscopy analysis were mechanically polished and then etched in a solution consisting of 2 ml of HF, 6 ml of HNO_3, 92 ml of Distilled Water. The worn surfaces after sliding wear tests were also examined using scanning electron microscope (SEM).

* Corresponding author. Tel.: +91 9493040920; fax: +91 8702459547.
E-mail address: srinivasu@nitw.ac.in (S.G. Setti).

0261-3069/$ - see front matter © 2013 Elsevier Ltd. All rights reserved.
http://dx.doi.org/10.1016/j.matdes.2013.03.107

Table 1
Chemical composition of the Ti–10V–4.5Fe–3Al alloy.

	Elements (weight%)								
	V	Al	Fe	O	N	P	C	S	Ti
Ti–10V–4.5Fe–3Al	9.6–10	3–3.2	4–5	0.11	0.009	0.01	0.02	0.001	Rest

2.3. Wear test

The dry sliding wear tests were conducted using a pin-on-disc (POD) wear testing apparatus (model: TR20-LE, Wear and Friction Monitor, Ducom Make, Bangalore, India). Cylindrical pins are of 8 mm diameter and 30 mm length were machined from the material treated for this condition. The wear tests were conducted according to ASTM G99 standard. The cylindrical pins were slide against disc of 165 mm diameter and 8 mm thick, EN-31 hardened to 60HRc, ground to surface roughness 1.6Ra (Fig. 1). The applied load varied from 3 kgf to 9 kgf at a constant speed of 500 rpm. The track diameter also varies from 40 mm to 120 mm. The samples were cleaned with acetone and weighed (up to an accuracy of 0.01 mg using microbalance) prior to and after each test in order to calculate the %weight loss.

The temperature rise and friction force were recorded from the digital display interfaced with the wear test machine. In order to record the temperature, the bare end of a thermocouple is placed on the pin is 1 mm above from the contact surface. In these tests, the temperatures recorded are the temperature of the position at which thermocouple is kept; actual temperatures at the contacting surface would be more than the recorded ones.

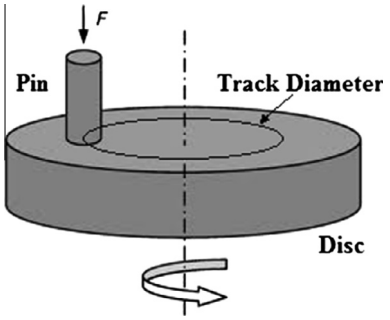

Fig. 1. Schematic diagram of pin-on-disc test setup.

3. Results and discussion

3.1. Effect of α + β solution treatment temperature on microstructure

Fig. 2 shows the backscattered electron image of α + β solution treated specimens at 680 °C, 720 °C and 750 °C respectively. Uniform distribution of equiaxed α particles in the continuous β phase is observed. The amount of α – phase present in the β – phase decreases with the increase of solution treatment temperature.

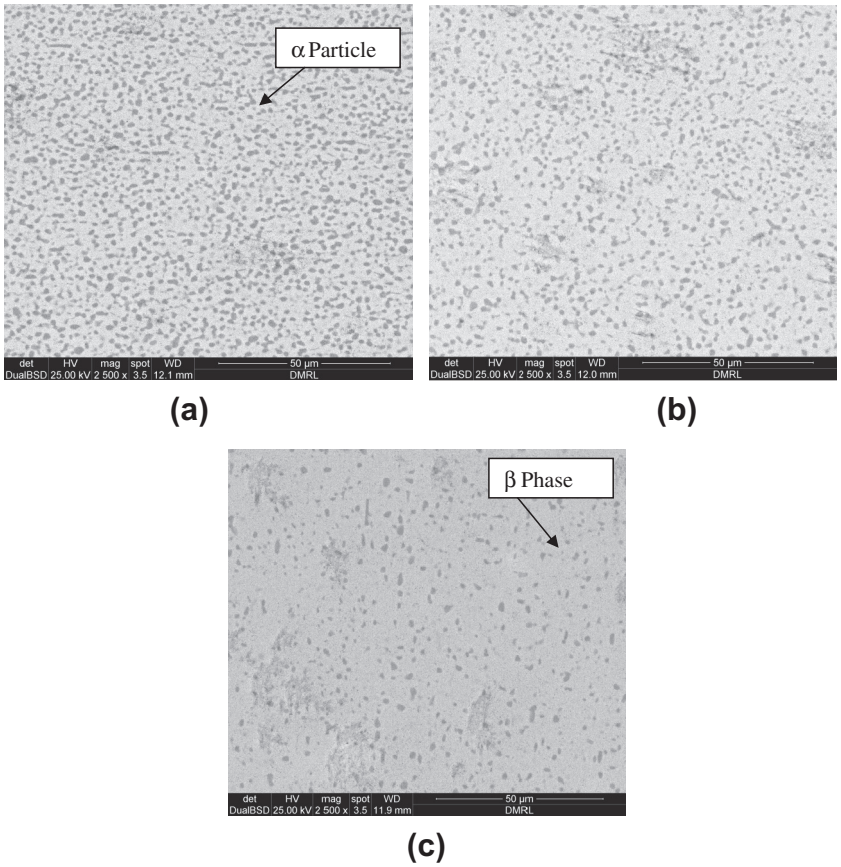

Fig. 2. SEM images of Ti alloy at three different α + β solution treatments (a) 680, (b) 720 and (c) 750 °C.

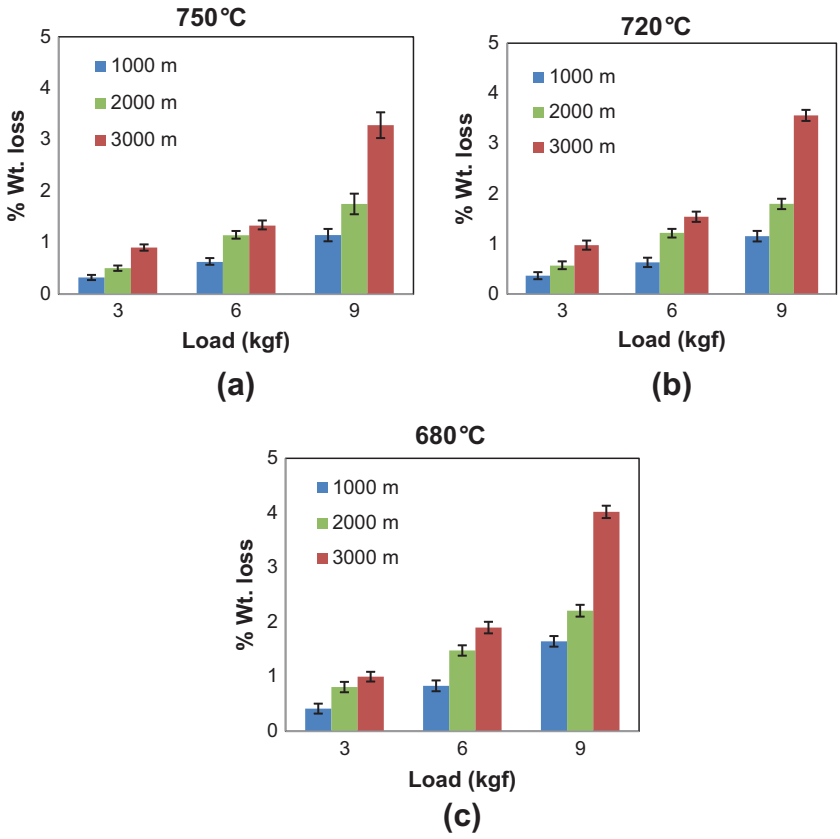

Fig. 3. %weight loss as a function of load and sliding distance at different α + β solution treatment temperatures.

3.2. Effect of α + β solution treatment temperature on sliding wear behaviour

3.2.1. %Weight loss

The %weight loss of the alloy as a function of sliding distance and loads for different α + β solution treatment temperatures are depicted in Fig. 3. At 750 °C β solution treatment temperature and 3 kgf load, the %weight loss at 1000, 2000 and 3000 m sliding distances are 0.33, 0.51 and 0.91 respectively. Similarly at 750 °C β solution treatment temperature and 9 kgf load, the %weight loss at 1000, 2000 and 3000 m sliding distances are 1.15, 1.75 and 3.28 respectively. It can be noticed from these points that the %weight loss increasing with the increase in sliding distance and load. Similar behaviour is observed in all other α + β solution treatments. With increase in applied load, the penetration of hard asperities of the counter surface to the softer pin surface increases and also the deformation and fracture of asperities of the softer surface increases. Again, on the other hand, more amount of softer material from the pin surface get accumulated at the valleys between the asperities on counter surface resulting in a decrease in the asperity height of the counter surface. This leads to a diminution in cutting efficiency of counter surface asperities. Again, surface and subsurface deformation and micro-cracking tendency increases with an increase in applied load. The effective wear from the specimen surface is due to the combined effect of all these above mentioned factors.

It is observed in Fig. 3 that, the %weight loss is increased gradually with sliding distance at 3 and 6 kgf loads, but at 9 kgf load it increases rapidly after 6 kgf load. In the initial stage, wear is mainly due to fragmentation of the asperities and removal of material due to cutting and flow of penetrating hard asperities into the softer surface. As time progresses, the frictional heating increases and due to the adiabatic type of heating temperature rises monotonically with sliding distance, higher temperature leads softening of the surface materials and the asperity contacts are deformed readily. Because of collective action of the load and sliding distance subsurface micro-cracks are generated which finally leads to removal of wear debris, especially from asperity contacts. As a result, it is expected that the %weight loss will increase with increase in sliding distance.

The %weight loss as a function of load and α + β solution treatment temperature at various sliding distances is shown in Fig. 4. It is clearly observed from the figure that, the %weight loss decreases with increasing the α + β solution treatment temperature. This is due to the fact that, the volume fraction of α decreases with the increase in the α + β solution treatment temperature. Since α is soft as compared to β, decreasing solution treatment leads to increasing volume fraction of softer phase and hence higher wear rate. It is observed from Fig. 4 that, the %weight loss of 720 and 750 °C solution treated samples showed almost same magnitude.

3.2.2. Coefficient of friction

Sliding wear is related to asperity-to-asperity contact of the two counter surfaces, which are in relative motion against each other. In the beginning the asperities are sharper and harder, because of the greater degree of sharpness of the asperities, the higher amount of stress acts on the asperity contact. Hence originally the coefficient of friction is high and it decreases with the increase in sliding distance as the asperities become blunt (Fig. 5). Fig. 5 shows the coefficient of friction as a function of load and sliding distance at different α + β solution treatment temperatures. At 750 °C solution treatment temperature (Fig. 5a) and 3 kgf load, the COF at 1000, 2000 and 3000 m sliding distances are 0.451, 0.423 and 0.417 respectively. Initially the COF is high at 1000 m

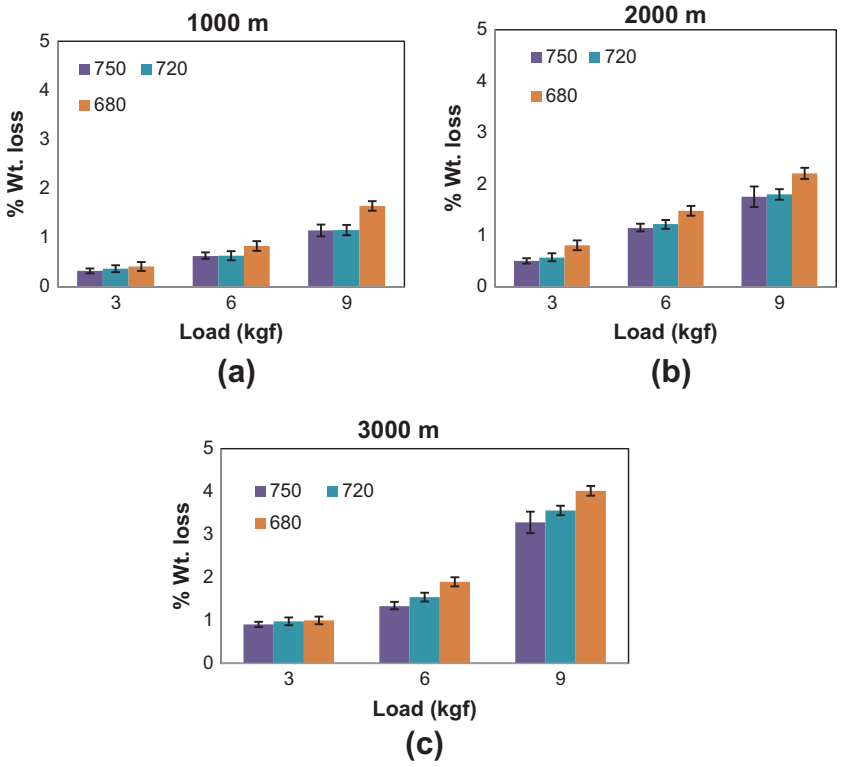

Fig. 4. %weight loss as a function of load and α + β solution treatment temperature at different sliding distances at (a) 1000 m; (b) 2000 m and (c) 3000 m.

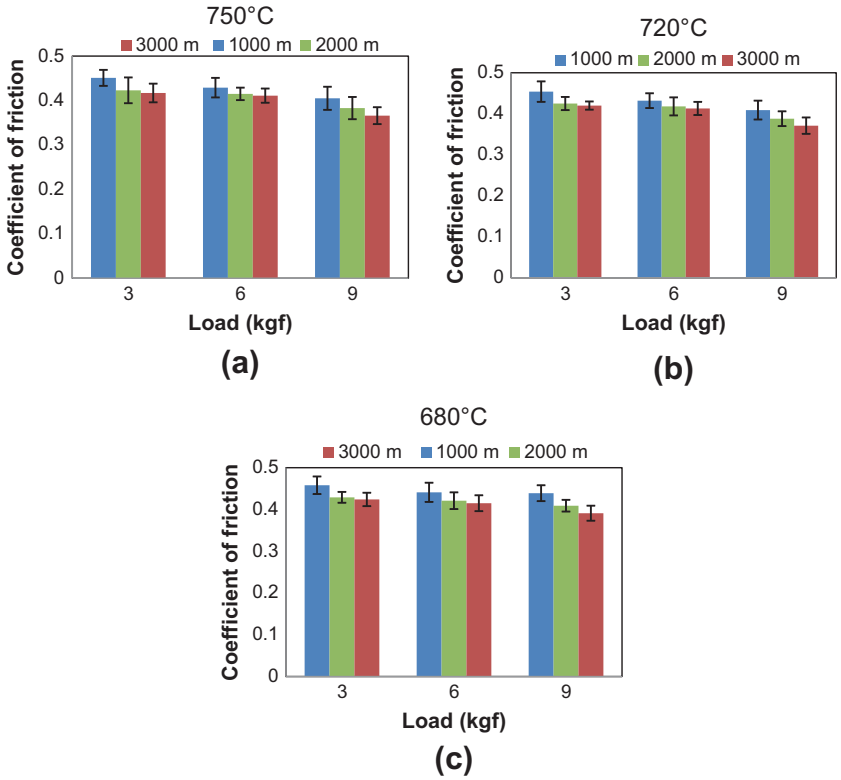

Fig. 5. Coefficient of friction as a function of sliding distance and load at different α + β solution treatment temperatures.

sliding distance and up to 2000 m sliding distance it is decreased significantly and remains almost constant further (at 3000 m). In the same way, at 750 °C solution treatment temperature and 9 kgf load, the %weight loss at 1000, 2000 and 3000 m sliding distances are 0.405, 0.383 and 0.366 respectively. From Fig. 5 it is observed that the coefficient of friction decreases with the increase in load. The asperities are getting deformed because of higher load, hence the decrease in sharpness resulting in decreasing the

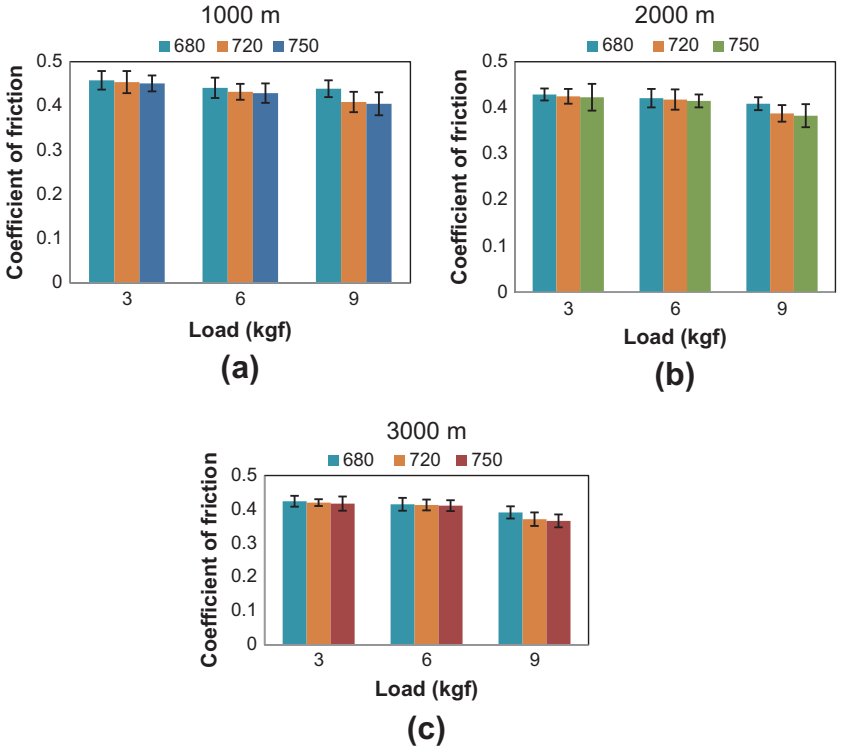

Fig. 6. Coefficient of friction vs load, α + β solution treatment temperature graphs at different sliding distances at (a) 1000 m; (b) 2000 m and (c) 3000 m.

coefficient of friction. Similar behaviour is observed in other α + β solution treatment temperatures.

Fig. 6 shows the coefficient of friction vs load at different α + β solution treatment temperatures. At 1000 m sliding distance and 3 kgf load, the coefficient of friction at 650, 680, 720 and 750 °C solution treatments are 0.46, 0.458, 0.454 and 0.451 respectively. Hence coefficient of friction is decreasing with the increase in α + β solution treatment temperature. If the amount of α is more, during the sliding more amount of α is filling the asperities due its soft nature and lead to reduce the coefficient of friction. At all loads similar behaviour is observed.

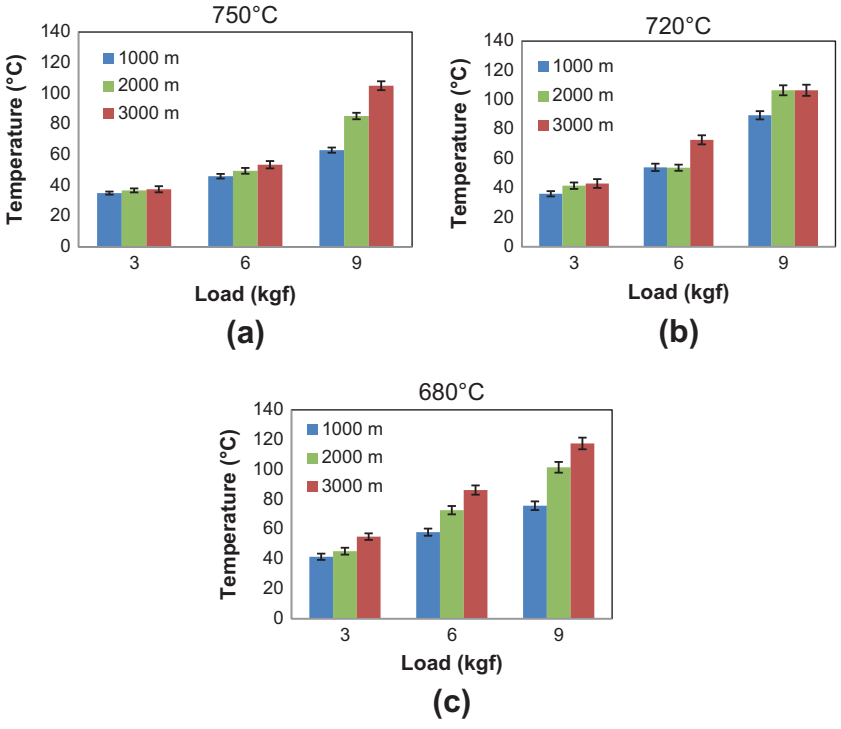

Fig. 7. Temperature vs load, sliding distance graphs at different α + β solution treatment temperatures.

3.2.3. Temperature

Temperature verses load for different sliding distances and different α + β solution treatment temperatures are shown in Fig. 7. At 750 °C β solution treatment temperature (Fig. 7a) and 1000 m sliding distance, the temperature developed at the interface between the pin and disc at 3, 6 and 9 kgf loads are 35, 46 and 63 °C respectively. In a similar fashion, at 750 °C β solution treatment temperature (Fig. 7a) and 3000 m sliding distance the temperature developed at 3, 6 and 9 kgf loads are 37.5, 53.5 and 105 °C respectively.

It can be noted that the temperature at the contact between the pin and disc increases with increase in sliding distance and load. Similar behaviour is observed in all α + β solution treatment conditions (Fig. 7b–d). During sliding a fraction of energy is spent on plastic deformation and subsequently material removal is also associated with considerable amount of energy overcoming the frictional force, which leads to heating of the contact surfaces. Thus the temperature increases with the increase in sliding distance.

Fig. 8 shows the temperature as a function of load for α + β solution treatment temperatures at different sliding distances. It is observed that, the temperature decreases with increase in α + β solution treatment temperature. Similar trends are observed in all other solution treated conditions (Fig. 8b–d). This is due to increase α + β solution treatment temperature results in decreasing volume fraction of softer α and increase in volume fraction of harder β, it is also associated with decreasing weight loss.

3.3. Worn surface analysis

Fig. 9 shows the fracture surface at three different loads and two different magnifications. Fig. 9a and b represents the worn surfaces of the at low load (3 kgf) in lower and higher magnifications respectively. The direction of sliding shown by an arrow. The debris on the surface is shown by a letter A in Fig. 9b. Due to continuous sliding, the formation of smooth continuous groves observed in all the micrographs (marked by B). Fig. 9c and d shows the SEM image of worn surfaces at medium load (6 kgf) in lower and higher magnifications respectively. The analysis of worn surfaces is in consistent with the work of Mujumdar et al. [14]. It clearly seen from the graphs that the amount of debris is more in the medium load conditions. At higher loads (9 kgf) the worn surfaces are shown in Fig. 9e and f at lower and higher magnifications respectively. With the increase in load, the flow of the material can be observed in Fig. 9e. This is due to the application of higher load (marked by C).

3.4. ANOVA Analysis

The ANOVA table consists of the terms such as degree of freedom, sum of squares, mean squares *F*-characteristic and percentage contribution *P*. The procedure for calculation of ANOVA is explained below.

Step 1:	Level totals and their averages A = Corresponding outputs at a particular level (1 + 2 + 3 + 4 + 5 + 6 + 7 + 8 + 9)	(1)
Step 2:	T = Sum of all the outputs	(2)
Step 3:	Correlation Factor (CF) = $(T^2)/n$; where n is the total number of experiments	(3)
Step 4:	Total sum of squares (St) = Sum of squares of outputs (Y_1^2 Total) – CF	(4)
Step 5:	Factor sum of squares (Sf) = $(((A_1^2)/nA_1) + ((A_2^2)/nA_1) + ((A_3^2)/nA_1)) - CF$ Where nA_1 is the number of experiments at level 1	(5)
Step 6:	Total and factor degree of freedom (DOF) = Total number of test runs – 1	(6)
Step 7:	Mean squares (MS) = Sum of squares/degree of freedom	(8)
Step 8:	Factor F ratios (F) = Sum of squares/Mean squares of error	(9)
Step 9:	Percentage contributions (%P) = Sum of squares/Total sum of squares	(10)
Step 10:	Formulate the final table	

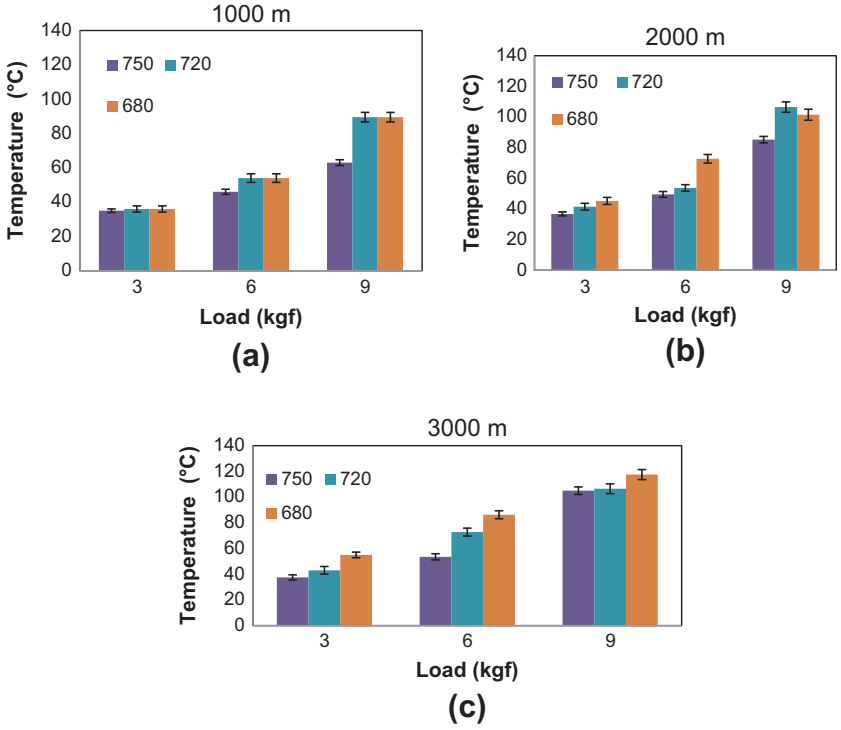

Fig. 8. Temperature vs load, α + β solution treatment temperature different sliding distances at (a) 1000 m; (b) 2000 m and (c) 3000 m.

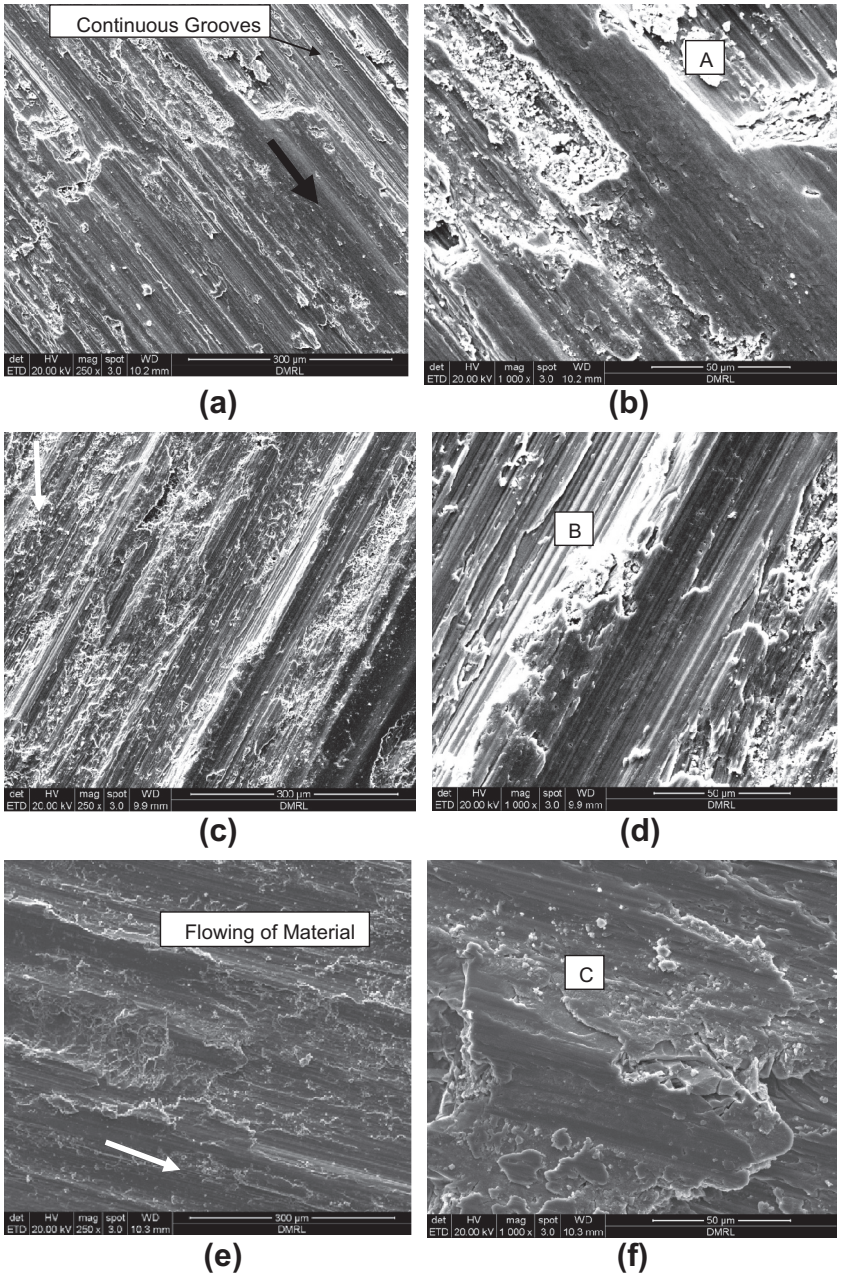

Fig. 9. Worn surfaces of the titanium alloy at three different loads (a and b) 3 kgf at 250× and 1000×; (c and d) 6 kgf at 250× and 1000×; and (e and f) 9 kgf at 250× and 1000×.

3.4.1. ANOVA for %weight loss

The analysis of variance is used to investigate which design parameters that significantly affect the quality characteristic. Table 2 shows the full factorial ANOVA analysis for the %weight loss. The most significant factor that affects the %weight loss is load (54.5%) followed by the track diameter (28.3%) and α + β solution treatment temperature (4.3%). As regards the effect of interactions, the load and track diameter (4.8%) followed by temperature and load interaction (0.3%) and temperature and track diameter (0.05%). The error percentage is 7.7%.

Table 2
The full factorial ANOVA analysis for the %weight loss.

Parameters	DOF	Sum of squares	Mean squares	*F*	*P*
Temp (A)	2	1.150	0.575	2.22	4.3
Load (B)	2	14.555	7.278	28.08	54.5
Track (C)	2	7.549	3.774	14.56	28.3
A × B	4	0.088	0.022	0.09	0.4
A × C	4	0.015	0.004	0.01	0.05
B × C	4	1.271	0.318	1.23	4.8
Error	8	2.073	0.259		7.65
Total	26	26.701			100.0

3.4.2. ANOVA for coefficient of friction

Table 3 shows the results of ANOVA analysis. It can be observed from the ANOVA analysis that the track diameter (p = 45.7%), normal load (p = 30.9%) and α + β solution treatment temperature (p = 14.9%) have great influence on coefficient of friction. The interactions α + β solution treatment temperature/normal load

Table 3
The results of ANOVA analysis.

Parameters	DOF	Sum of squares	Mean squares	*F*	*P*
Temp (A)	2	0.0020	0.0010	12.22	14.93
Load (B)	2	0.0041	0.0021	25.28	30.88
Track (C)	2	0.0061	0.0030	37.34	45.62
A × B	4	0.0003	7.702E−05	0.94	2.29
A × C	4	5.36E−05	1.341E−05	0.16	0.40
B × C	4	0.0002	3.357E−05	0.41	1.00
Error	8	0.0007	8.212E−05		4.88
Total	26	0.0135			100.00

Table 4
The ANOVA results of temperature.

Parameters	DOF	Sum of squares	Mean squares	*F*	*P*
Temp (A)	2	2536.01	1268.00	18.95	13.76
Load (B)	2	12253.92	6126.96	91.55	66.51
Track (C)	2	2610.03	1305.02	19.49	14.17
A × B	4	151.87	37.97	0.57	0.82
A × C	4	77.24	19.31	0.29	0.42
B × C	4	259.53	64.88	0.96	1.41
Error	8	535.42	66.93		2.91
Total	26	18424.02			100.00

(p = 2.3%), normal load/track diameter (p = 1%) and α + β solution treatment temperature/track diameter (p = 0.4%) have relatively less significance. Finally the error is 4.9%.

3.4.3. ANOVA for temperature

Table 4 shows the ANOVA results of temperature. The normal load factor (p = 66.5%) has a significant influence on the temperature of the alloy while the track diameter (p = 14.16%) and α + β solution treatment temperature (p = 13.8%) have a relatively lesser impact. The interactions α + β solution treatment temperature/normal load (p = 0.82%), normal load/track diameter (p = 1.4%) and α + β solution treatment temperature/track diameter (p = 0.4%) have significantly lesser influence.

4. Conclusions

The following conclusions can be drawn from the present study are:

- The volume fraction of α increases with decrease in α + β solution treatment temperature.
- The %weight loss decreased with increasing α + β solution treatment temperature.
- For particular load COF decreased with increasing sliding distance. The coefficient of friction decreased with increasing in the α + β solution treatment temperature.
- The temperature developed at the pin and disc interface decreased with the increase in α + β solution treatment temperature.
- The most significant factor that influenced the %weight loss was load (p = 54.5%) followed by the track diameter (p = 28.3%) and α + β solution treatment temperature (p = 4.3%).
- The track diameter (p = 45.7%), normal load (p = 30.9%) and α + β solution treatment temperature (p = 14.9%) had a great influence on coefficient of friction.
- The normal load factor (p = 66.5%) had a significant influence on the temperature of the alloy while the track diameter (p = 14.16%) and α + β solution treatment temperature (p = 13.8%) had a minor effect.

References

[1] Leyens C, Peters M. Titanium and titanium alloys – fundamentals and applications. KGaA, Weinheim: WILEY-VCH Verlag GmbH & Co; 2003.
[2] Moiseyev Valentin N. Titanium alloys – Russian aircraft and aerospace applications. Taylor & Francis Group: CRC Press; 2006.
[3] Boyer RR. An overview on the use of titanium in the aerospace industry. Mater Sci Eng A 1996;213:103–14.
[4] Yamada Makoto. An overview on the development of titanium alloys for non-aerospace application in Japan. Mater Sci Eng A 1996;213:8–15.
[5] Zhou YG, Zeng WD, Yu HQ. An investigation of a new near-beta forging process for titanium alloys and its application in aviation components. J Mater Process Technol 2011;211:1400–8.
[6] Gorynin IV. Titanium alloys for marine application. Mater Sci Eng A 1999;263:112–6.
[7] Schutz RW, Watkins HB. Recent developments in titanium alloy application in the energy industry. Mater Sci Eng A 1998;243:305–15.
[8] Gabriel SB, Panaino JVP, Santos ID, Araujo LS, Mei PR, de Almeida LH, et al. Characterization of a new beta titanium alloy, Ti–12Mo–3Nb, for biomedical applications. J Alloy Compd 2012;536S:S208–10.
[9] Budinski KG. Tribological properties of titanium alloys. Wear 1991;151(203):17.
[10] Molineri A, Straffelini G, Tesi B, Baccai T. Dry sliding wear mechanism of the Ti6Al4V alloy. Wear 1997;208(105):12.
[11] Masmoudi M, Assoul M, Wery M, Abdelhedi R, El Halouani F, Monteil G. Wear behaviour of nitric acid passivated cp Ti and Ti6Al4V. J Alloy Compd 2009;478:726–30.
[12] Dong H, Bell T. Tribological behaviour of aluminium sliding against Ti6Al4V in unlubricated contact. Wear 1999;225–229(874):84.
[13] Majumdar P, Singh SB, Chakraborty M. The influence of heat treatment and role of boron on sliding wear behaviour of β-type Ti–35Nb–7.2Zr–5.7Ta alloy in dry condition and in simulated body fluids. J Mech Behav Biomed Mater 2011;4:284–97.
[14] Majumdar P, Singh SB, Chakraborty M. Wear response of heat-treated Ti–13Zr–13Nb alloy in dry condition and simulated body fluid. Wear 2008;264:1015–25.
[15] Li SJ, Yang R, Li S, Hao YL, Cui YY, Niinomi M, et al. Wear characteristics of Ti–Nb–Ta–Zr and Ti–6Al–4V alloys for biomedical applications. Wear 2004;257:869–76.
[16] Siddhartha, Patnaik Amar, Bhatt Amba D. Mechanical and dry sliding wear characterization of epoxy–TiO_2 particulate filled functionally graded composites materials using Taguchi design of experiment. Mater Des 2011;32:615–27.
[17] Sahin Y. Optimal testing parameters on the wear behaviour of various steels. Mater Des 2006;27:455–60.
[18] Mahapatra SS, Patnaik Amar. Study on mechanical and erosion wear behavior of hybrid composites using Taguchi experimental design. Mater Des 2009;30:2791–801.
[19] Das Suman Kalyan, Sahoo Prasanta. Tribological characteristics of electroless Ni–B coating and optimization of coating parameters using Taguchi based grey relational analysis. Mater Des 2011;32:2228–38.
[20] Basavarajappa S, Chandramohan G, Paulo Davim J. Application of Taguchi techniques to study dry sliding wear behaviour of metal matrix composites. Mater Des 2007;28:1393–8.
[21] Yolton CF, Froes FH, Malone RF. Alloy element effects in metastable titanium alloy. Metall Trans A 1979;10:132–4.